Available online at www.sciencedirect.com

ScienceDirect

Coordination Chemistry Reviews 251 (2007) 1663–1677

COORDINATION CHEMISTRY REVIEWS

www.elsevier.com/locate/ccr

Review

Transition-metal sensitised near-infrared luminescence from lanthanides in d–f heteronuclear arrays[☆]

Michael D. Ward [*]

Department of Chemistry, University of Sheffield, Sheffield S3 7HF, UK

Received 15 September 2006; accepted 21 October 2006
Available online 26 October 2006

Contents

Abstract

This review summarises recent work from several groups on the preparation and photophysical properties of d–f heteronuclear assemblies in which a strongly light absorbing d-block chromophore is used as an antenna group to generate sensitised luminescence from near-infrared emitting lanthanide(III) centres (especially Yb, Nd, Er) following d → f photoinduced energy-transfer. An introduction summarises the technological importance of near-IR luminescence, the problems associated with its sensitisation and the resultant short lifetimes, and how these might be overcome. The next section describes work in this field from other groups; the last reviews work from the authors own group on (i) polypyridine-bridged d–f complexes and (ii) cyanide-bridged d–f coordination networks, with an emphases on both molecular design and synthesis, and understanding the photophysical properties such as the efficiency of d → f photoinduced energy-transfer.

Keywords: Transition metals; Lanthanides; Luminescence; Photophysics; Energy-transfer; Near infrared

1. Introduction and background

The last few years has seen great interest amongst coordination chemists in the study of complexes of those members of the lanthanide(III) series which show luminescence in the near-infrared (NIR) region. Strong luminescence in the visible region, from Tb(III) and Eu(III) in particular, is very well known and widely exploited in applications such as lighting and display devices – from the humble fluorescent light to OLEDs [1] – as well as sensors in which the luminescence intensity and/or lifetime are sensitive to a specific substrate [2], and biological imaging and assays based on resonance energy-transfer between a chromophore and the metal ion [3].

Near-infrared luminescence is also of technological interest, for two completely different reasons. Firstly, telecommunications optical networks based on silica fibres use NIR radiation (in the range *ca.* 1–1.6 μm) to send information because in this region silica has a high transparency. In particular the emission lines of Pr(III) at 1.3 μm ($^1G_4 \rightarrow {}^3H_5$) and Er(III) at 1.5 μm ($^4I_{13/2} \rightarrow {}^4I_{15/2}$) match well the 'windows of transparency' in silica and are consequently used in optical amplifiers for fibre-optic networks. Secondly, human tissue is relatively transparent at around 0.8–1 μm. In the visible region the absorbance is high principally because of porphyrin chromophores; further into the NIR region the absorbance is high because of O–H vibrational overtones from water. Metal ions which are luminescent in this

---

[☆] Based on a keynote lecture presented at the 37th International Conference on Coordination Chemistry, 13–18 August 2006, Cape Town, South Africa.

[*] Tel.: +44 114 2229484; fax: +44 114 2229346.
E-mail address: m.d.ward@Sheffield.ac.uk.

0010-8545/$ – see front matter © 2006 Elsevier B.V. All rights reserved.
doi:10.1016/j.ccr.2006.10.005

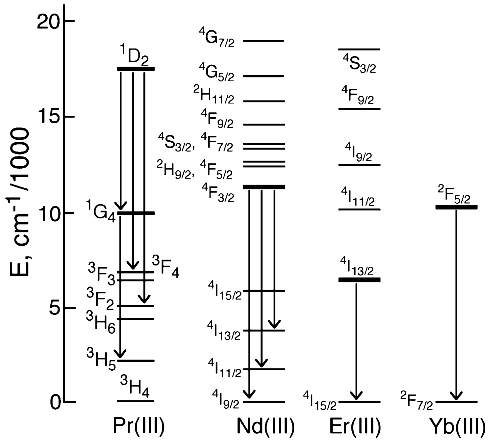

Fig. 1. Diagram of the f–f energy levels of Pr(III), Nd(III), Er(III) and Yb(III) up to *ca.* 20,000 cm^{-1}. The energy levels from which NIR luminescence originates are marked in bold, and the main NIR emissions are shown as descending arrows.

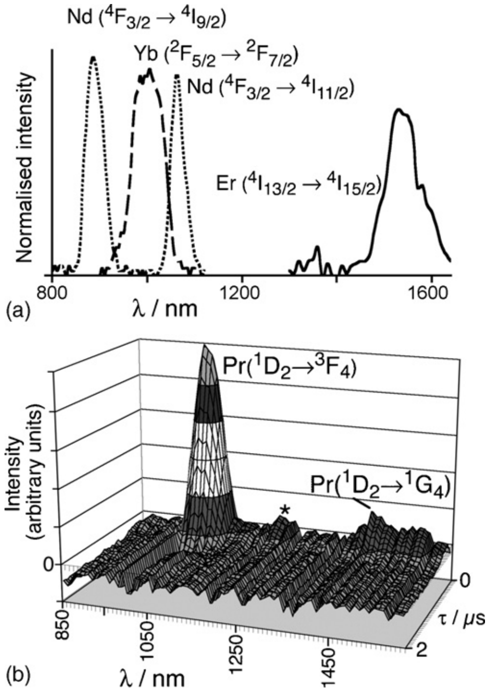

Fig. 2. (a) Typical steady-state emission spectra of Nd(III), Yb(III) and Er(III) complexes; (b) a typical time-resolved emission spectrum of a Pr(III) complex (the feature marked * is an artefact).

intermediate region, such as Yb(III) at 980 nm and Nd(III) at 880 nm, are ideal candidates for in vivo luminescent imaging since their emission can be detected through a considerable thickness of tissue. Both of these issues have been known for a long time. However, recent advances in electronics and detector technology mean that time-resolved luminescence measurements in the NIR region – which is inherently very weak because of the ease with which low energy excited states can be quenched by molecular vibrations – can be performed using readily available and modestly priced equipment, and this must be an important factor in the recent popularity of the field amongst coordination chemists. The relevant energy levels for the most widely studied NIR-luminescent lanthanides, Pr(III), Nd(III), Er(III) and Yb(III), are in Fig. 1, with the main luminescent transitions in the NIR region indicated; typical luminescence spectra are in Fig. 2.

From a photophysical point of view there are two distinct problems to overcome to achieve relatively intense and long-lived luminescence from lanthanides in the NIR region. (From a chemical point of view there may of course be many other problems associated with design and synthesis!) These are: (i) generating the excited state in the first place, given the very low absorption coefficients of Laporte-forbidden f–f transition; (ii) preventing the rapid deactivation of the excited state by the vibrations of the ligands and/or solvent molecules. The second of these issues has been the target of attention from several groups and has been tackled in various quite different ways. The imido-diphosphinate ligand $Ph_2P(O)–(N^-)–PPh_2(O)$ (‘idp’), a sterically crowded *O*,*O*-donor chelate, forms Ln(idp)$_3$ complexes in which the 12 phenyl substituents protect the metal from solvent interactions and in which there are no high-energy oscillators close to the metal, resulting in unusually long near-IR luminescence lifetimes (Yb, 50 μs; Er, 6 μs; Nd, 2.7 μs) [4]. Perfluorination of the phenyl rings to give Ln(Fidp)$_3$ [Fidp = $(C_6F_5)_2P(O)–(N^-)–P(C_6F_5)_2(O)$] gives astonishingly large additional increases in luminescence lifetimes (*e.g.* Er up to 200 μs) due to removal of all CH oscillators from the compound, showing clearly that CH oscillators which are ‘remote’ from the metal centre can make an important contribution to quenching [5]. An alternative approach from Piguet’s group was to prepare Cr(III)–Ln(III) and Ru(II)–Ln(III) dinuclear complexes in which remarkably long-lived luminescence from Yb(III), Nd(III) and Er(III) occurred as a consequence of rate-limiting energy-transfer from the excited-state of the d-block component [6,7]. Van Veggel and co-workers have shown how doping luminescent lanthanide ions into soluble LaF_3 or $LaPO_4$ nanoparticles results in luminescence lifetimes that are orders of magnitude longer than those observed for conventional coordination complexes [8]. Thus there are many ways in which the issue of short lifetimes and low intensity for NIR luminescence might be overcome.

It is the first of the above-mentioned issues however – how to sensitise the excited state in the first place – which is the focus of this review. It has been well known for many years that an effective mechanism for overcoming the low light absorbance of Ln(III) ions is to use aromatic ligands with fully allowed π–π^* transitions [9]. Excitation of a ligand-centred transition, usually in the UV region, is followed by fast energy-transfer (usually, but not always [10], from the triplet excited state of the ligand) to the lanthanide centre which becomes itself excited, leading to strong luminescence by using the organic chromophores as light-harvesting groups. The only significant limitation of this is that it becomes more difficult to find ligand-centred chromophores at wavelengths longer than the UV. The low-energy emissive states of Nd(III), Er(III) and Yb(III), at *ca.* 11,300, 10,200 and 6500 cm^{-1}, respectively, above their ground states, could in principle be populated by triplet energy-donors with energies of *ca.* 2000 cm^{-1} greater than this, *i.e.* in the red region of the spectrum for Nd(III) and the NIR region for the other two (a smaller gradient than this for energy-transfer is likely to result in deleterious thermally activated back energy-transfer at room temperature). In addition to being less wasteful of energy – using 250 nm excitation to generate 1530 nm luminescence from Er(III) seems extravagant and inelegant – there are obvious advantages to using longer wavelengths for sensitisation of NIR luminescence. For example in biological probes the excitation radiation needs to be able to penetrate the tissue in order to generate the luminescence from the probe in the first place, which rules out UV excitation (and also much of the visible region). An elegant solution to this recently has been to use two-photon excitation of Eu(III) or Tb(III) complexes such that excitation at *ca.* 800 nm results in the characteristic visible luminescence [11,12].

There are a few examples of chromophores which absorb at longer wavelengths, in the visible region, being built into ligands and used as sensitisers of NIR luminescence (compounds **I–IV**). Van Veggel and co-workers used ligands containing fluorescein-based and related chromophores (*e.g.* **I**), which absorb in the 500–600 nm region, which allow visible-light sensitisation of NIR luminescence from lanthanides [10,13,14]; the author's group used a tetrazine-based ligand which has an absorption maximum at 503 or 524 nm in mono- and dinuclear lanthanide complexes (*e.g.* **II**), respectively [15]; and Parker's group used a Pd(II)-porphyrin chromophore to achieve sensitised, circularly polarised luminescence from a covalently attached chiral Yb(III) macrocyclic complex in **III** [16]. Very recently Ziessel, Bünzli and co-workers used a bora-diazaindacene dye, with an extinction coefficient of 65,000 M^{-1} cm^{-1} at 529 nm, as sensitiser of NIR luminescence from Yb(III), Nd(III) and Er(III) in **IV** [17].

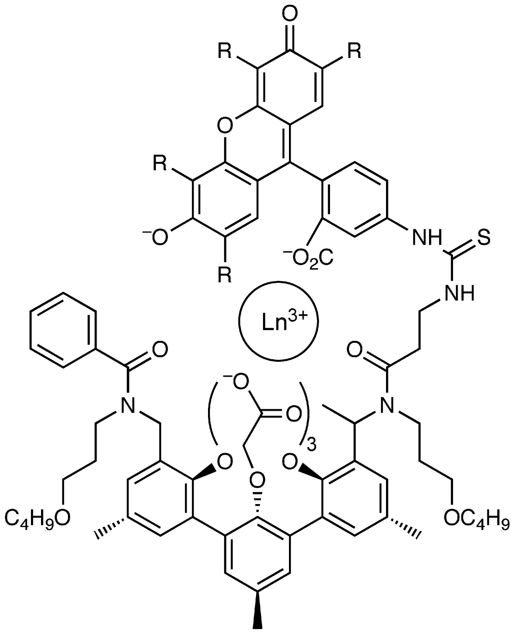

I (R = H, Br, I; see ref. 13)

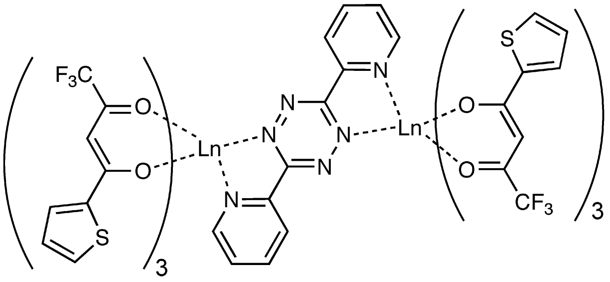

II (Ln = Yb, Er; see ref. 15)

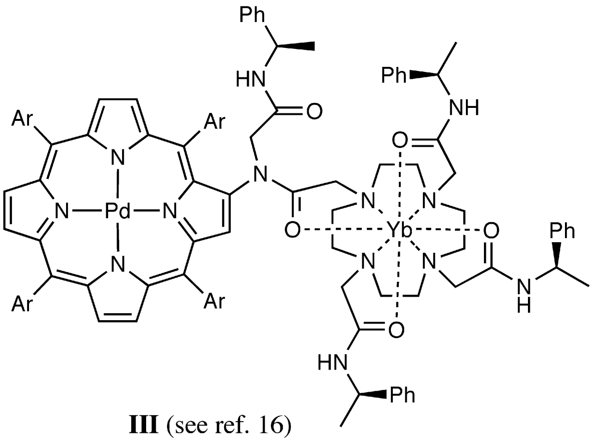

III (see ref. 16)

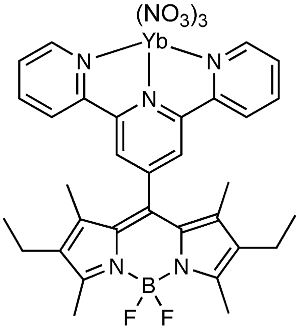

IV (see ref. 17)

However the best source of strongly absorbing chromophores spanning the visible region is the d-block, where stable complexes with long-lived excited states can be found at almost any desired wavelength. Transition-metal complexes can meet all of the following criteria:

(i) a strong absorption maximum which can be selected almost anywhere in the visible or NIR region;
(ii) a heavy metal ion which will facilitate inter-system crossing and give a high triplet quantum yield of the energy-donor following excitation;
(iii) relatively long-lived triplet excited states, which will facilitate energy-transfer to a covalently attached lanthanide;
(iv) kinetic inertness and photochemical stability;
(v) in many cases, luminescence from the (unquenched) triplet state allows energy-transfer to the lanthanide to be followed both by quenching of the donor as well as appearance of sensitized emission from the lanthanide;
(vi) synthetic convenience, *i.e.* the presence of a vacant coordination site at the periphery of the complex (‘complexes-as-ligands’) to which a lanthanide fragment can be attached.

All of these criteria have been extensively exploited in the field of supramolecular photochemistry of d-block metal fragments, and exactly the same set of properties makes the ideal as sensitisers for NIR lanthanide luminescence. Accordingly, this review summarises recent developments in the field of such ‘d–f’ complexes, which combine a d-block chromophore and a NIR-luminescent lanthanide. Section 2 summarises briefly relevant work from other groups; Section 3 then provides a more personal account of recent work from the author’s laboratory.

2. Work from other groups

The recent surge of interest in use of d-block complexes as sensitisers for lanthanide-based NIR luminescence began with a seminal paper by van Veggel and co-workers, published in 2000, in which the use of either ferrocene or $[Ru(bipy)_3]^{2+}$ units, covalently attached to Yb(III) or Nd(III) polycarboxylate units, was described (compounds **V** and **VI**) [18].

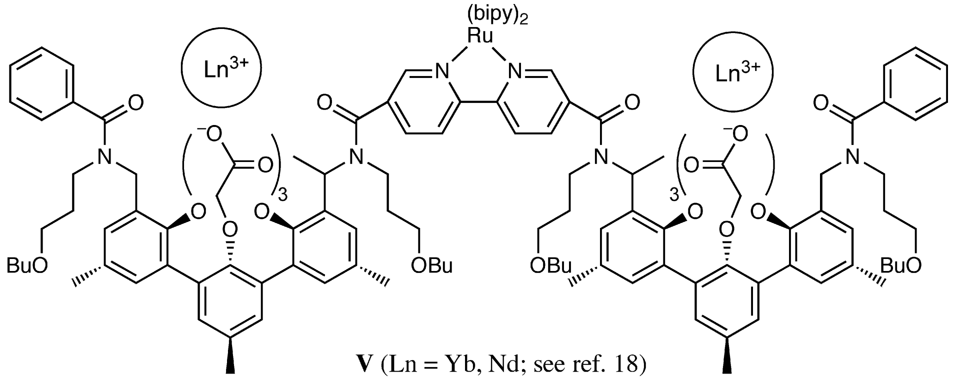

V (Ln = Yb, Nd; see ref. 18)

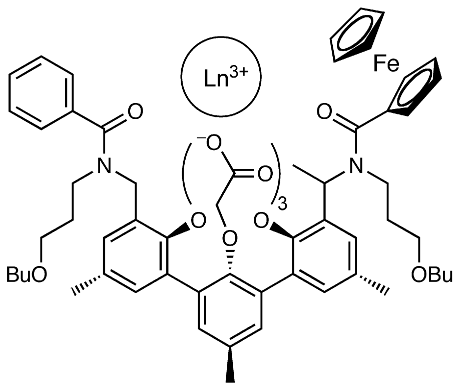

VI (Ln = Yb, Nd; see ref. 18)

The low-lying triplet state of ferrocene (*ca.* 13,300 cm^{-1}) in particular is a good match for the energy-accepting luminescent states of Nd(III) (11,300 cm^{-1}) and Yb(III) (10,200 cm^{-1}); the ^{3}MLCT state of $[Ru(bipy)_3]^{2+}$ at *ca.* 17,400 cm^{-1} is quite remote in energy from the Yb(III) excited state, but overlaps with many of the higher-lying Nd(III)-based states (such as $^4G_{5/2}$ at 17,100 cm^{-1} and several others just below this) which could act as initial energy-acceptors before internal conversion of Nd(III) to the emissive $^4F_{3/2}$ state. In both cases excitation of the d-block chromophore, at 320 or 440 nm for ferrocene, or 450 nm for $[Ru(bipy)_3]^{2+}$, resulted in the appearance of sensitised NIR luminescence from Nd(III) or Yb(III) with characteristic lifetimes in the microsecond domain. Not surprisingly on the basis of the matching between the donor and acceptor energy-levels, and donor/acceptor spectroscopic overlap, Ru → Yb energy-transfer was found to be inefficient and at least an order of magnitude slower than Ru → Nd energy-transfer, with rates of $\leq 10^5$ and $\approx 10^6\,s^{-1}$, respectively. These relatively slow energy-transfer rates are in addition a consequence of the high metal–metal separations, and the absence of a conjugated pathway between energy-donor and energy-acceptor which hinders any energy-transfer that is occurring via a double electron exchange (Dexter) process. It was noted that time-resolved luminescence measurements involving Yb(III) were problematic because the Yb(III)-based emission at 980 nm overlaps with the tail of the residual Ru(II)-based luminescence in complex **V**, such that there are two components with different lifetimes in this region. This is not such a problem with Nd(III) where the 1330 nm band can be used for lifetime measurements.

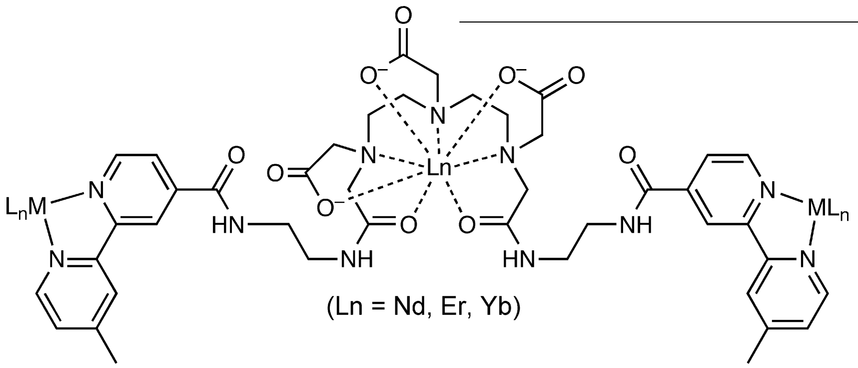

VII [ML$_n$ = *fac*-{Re(CO)$_3$Cl}]
VIII [ML$_n$ = {Ru(bipy)$_2$}$^{2+}$]
IX [ML$_n$ = {Os(bipy)$_2$}$^{2+}$]
(see refs. 19, 20)

Faulkner and co-workers have extended this principle to the use of other d^6 polypyridyl complexes of Ru(II), Re(I) and Os(II) as sensitisers in both covalently linked and non-covalently linked (supramolecular) polynuclear assemblies. The trinuclear complexes **VII–IX** contain two d-block Ru(II), Re(I) or Os(II) chromophores covalently linked to a Ln/DTPA fragment (Ln = Nd, Er, Yb) [19,20]. The presence of the lanthanide(III) ion in the DTPA binding site reduces the emission intensity of the d-block unit as a result of d → f energy-transfer, with a concomitant small reduction in the luminescence lifetime; sensitised Ln-based NIR emission was observed in every case following excitation of the d-block chromophore. The rates of d → f energy-transfer, estimated from the rise-times of the sensitised NIR luminescence, showed some surprising variations. In particular, Re → Ln energy-transfer was two orders of magnitude faster than Ru → Ln energy-transfer, despite the fact that [Re(bipy)(CO)$_3$Cl] and [Ru(bipy)$_3$]$^{2+}$ emit at very similar wavelengths such that Re/Ln and Ru/Ln donor/acceptor spectroscopic overlap is expected to be comparable for a given lanthanide. The difference was ascribed to conformational effects arising from electrostatic factors: electrostatic repulsion between the two Ru^{2+} sensitisers and the central Ln^{3+} fragment in **VIII** is likely to result in these flexible complexes adopting an opened-out conformation to maximise the Ru···Ln separation, whereas this effect will not occur with the neutral [Re(bipy)(CO)$_3$Cl] fragments in **VII**, allowing shorter Re···Ln separations. In addition, this work is notable for describing the first use of [Os(bipy)$_3$]$^{2+}$ as a sensitiser for lanthanides, which could allow excitation wavelengths as low as 700 nm (*i.e.* approaching the biologically useful window where tissue has high transparency) to be used. Os → Ln energy-transfer was faster than Ru → Ln energy-transfer, presumably because the lower energy ^{3}MLCT state of [Os(bipy)$_3$]$^{2+}$ provides better spectroscopic overlap with the lanthanide emissive state; note that electrostatic/conformational factors will be similar between the Ru$_2$Ln (**VIII**) and Os$_2$Ln (**IX**) series.

Similar combinations of sensitiser and luminophore were used in non-covalent assemblies by the same group [21]. The carboxylate group pendant from the d-block bipyridyl complexes **X–XII** binds in CH$_3$OH or CD$_3$OD solution to the lanthanide(III) centre of the seven-coordinate complexes **XIII** based on cyclen-triacetate, affording carboxylate-bridged supramolecular d/f dinuclear assemblies (Scheme 1) which show similar behaviour to the covalently linked analogues, *viz.* partial quenching of the d-block luminescence, and the appearance of sensitised NIR lanthanide-based luminescence, following selective excitation of the d-block component. A particular advantage of this method is that it allows numerous d/f combinations to be evaluated simply by mixing the component parts, without having to perform a 'covalent synthesis' of each combination separately. Addition of phosphate (a bidentate chelate to lanthanides) disrupts the carboxylate bridge and separates the components, switching off the d–f energy-transfer [22]. Beer et al. have also used demonstrated Ru → Ln energy-transfer in supramolecular assemblies of [Ru(bipy)$_3$]$^{2+}$ and lanthanide(III) components [23]. In these cases the [Ru(bipy)$_3$]$^{2+}$ antenna group is functionalised with one, two or six calixarene pendant groups (*e.g.* compound **XIV**); these can bind lanthanide(III) ions by virtue of their amide/carboxylate/phenol donor sets. Binding of Nd(III) ions in the calixarene cavities results in partial quenching of the [Ru(bipy)$_3$]$^{2+}$-based luminescence and the appearance of sensitised Nd(III)-based luminescence with a rate constant of $2.4 \times 10^6\,s^{-1}$.

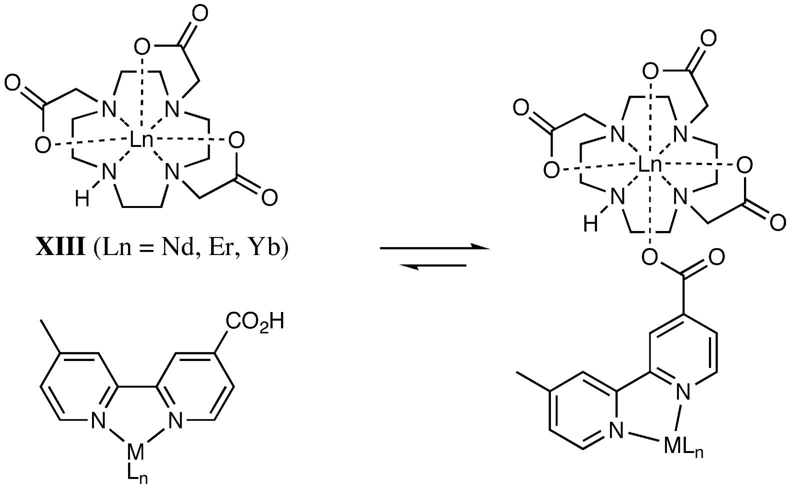

XIII (Ln = Nd, Er, Yb)

X [ML$_n$ = *fac*-{Re(CO)$_3$Cl}]
XI [ML$_n$ = {Ru(bipy)$_2$}$^{2+}$]
XII [ML$_n$ = {Os(bipy)$_2$}$^{2+}$]

Scheme 1.

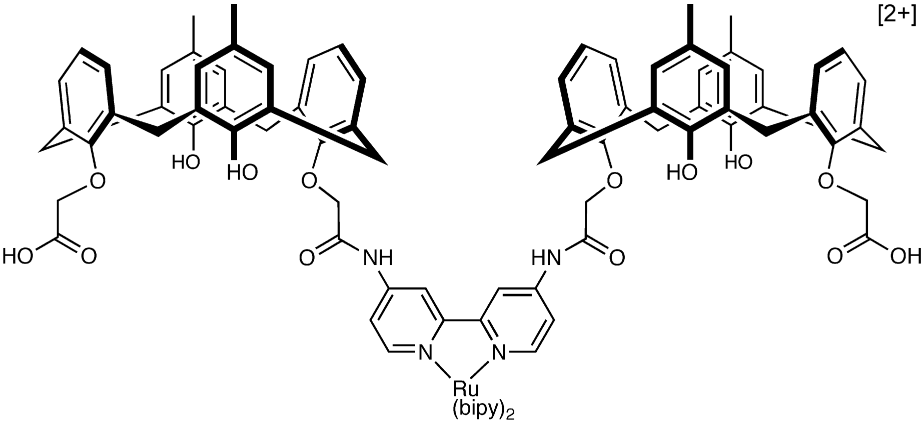

XIV (see ref. 23)

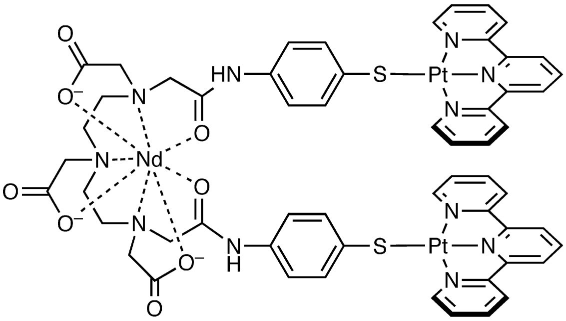

XV (see ref. 24)

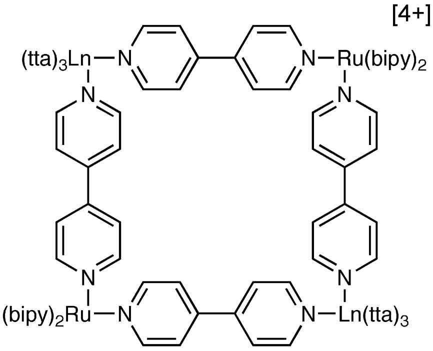

XVI (Ln = Nd, Yb; see ref. 25)

In complex **XV**, described by Pikramenou and co-workers, the Nd(III) ion fulfils two quite different roles. Folding up of the DTPA binding site around the lanthanide(III) ion results in the two planar Pt(II)-terpyridyl units becoming oriented on the same side of the complex to give a ‘hairpin’ structure in which both Pt(II)-terpyridyl units can intercalate into DNA simultaneously and stiffen the DNA backbone. In addition the Nd(III) ion acts as a luminescent reporter group, generating 1060 nm emission following excitation of the Pt(II) chromophores which have a strong LLCT (thiolate → terpyridyl) band at 515 nm that can act as a sensitiser for the NIR luminescence [24].

The ability of lanthanide tris-diketonates Ln(dik)$_3$ to bind two additional monodentate or one bidentate pyridine-type ligand to give eight-coordinate adducts ‘$Ln(dik)_3(NN)$’ has been exploited as a facile way of assembling d- and f-block components. Reaction of $[Ru(bipy)_2(4,4'\text{-}bipy)_2]^{2+}$ (which has two pendant pyridyl units at 90° to one another) with $Ln(tta)_3$ (Htta = 2-thenoyl-trifluoro-acetylacetone) affords the molecular squares **XVI** which were characterised on the basis of their mass spectra. Excitation of the Ru(II) chromophores at 420 nm afforded sensitised NIR luminescence from Nd(III) and Yb(III), with Nd(III) affording the greater degree of quenching of the Ru-based luminescence because Ru → Ln energy-transfer is faster to Nd(III) than to Yb(III), for reasons discussed earlier [25]. Similarly, binding of $Ln(hfac)_3$ (Hhfac = hexafluoroacetylacetone) units to the pendant bipyridyl or phenanthroline sites of complexes **XVII** and **XVIII** afforded Pt_2Ln_2 and Pt_2Ln_4 assemblies in which the MLCT transition of the Pt_2^{II} chromophore at 350–450 nm acted as sensitiser for NIR luminescence from Nd(III) and Yb(III) [and visible luminescence from Eu(III)] [26].

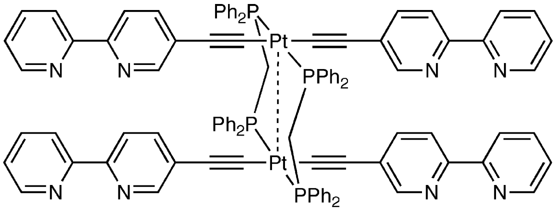

XVII (see ref. 26)

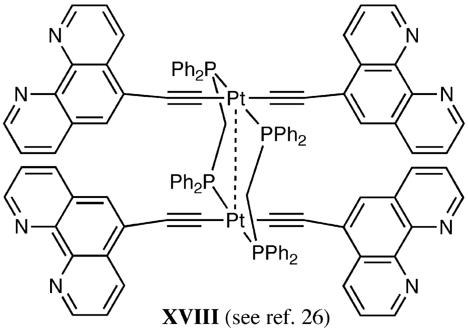

XVIII (see ref. 26)

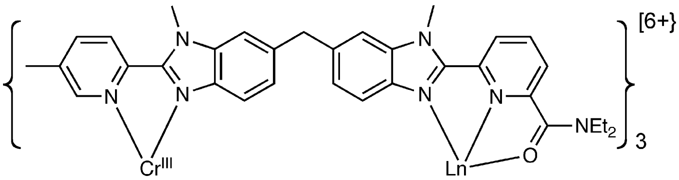

XIX (see ref. 6)

Piguet and co-workers have exploited the kinetic inertness of octahedral complexes of Cr(III) and Ru(II) to prepare, in a stepwise manner, d–f dinuclear complexes having a triple helical architecture. The d-block chromophore is held at the six-coordinate site, and a lanthanide(III) ion at the nine-coordinate site, within the helical array of three ligands (see *e.g.* structure **XIX**). Again these complexes show d–f energy-transfer with the d-block chromophore being able to sensitise luminescence from Nd(III), Er(III) and Yb(III). However a particularly interesting feature of these complexes is that the rate constant of the lanthanide-based luminescence is greater than the d–f energy-transfer rate-constant. Thus, the energy-transfer step is rate limiting and the NIR luminescence decay is driven by the rate at which the lanthanide excited state is populated by directional energy-transfer from the d-block ion. Since the energy-transfer is phonon-assisted (*i.e.* coupled to molecular vibrations), cooling the samples to 10 K results in very slow d–f energy-transfer and hence very long lifetimes for lanthanide-based emission. For example the luminescence lifetime of Yb(III) following sensitisation by Cr(III) can be varied between 23 μs in MeCN solution at 295 K, and 2 ms at 10 K. This remarkable observation may allow for the precise temperature-controlled tuning of NIR luminescence lifetimes [6,7].

Finally in this section, van Veggel and co-workers have examined sensitised NIR luminescence in nanoparticles doped with lanthanides. Colloidal particles of $LaVO_4$ can be rendered soluble in organic solvents by coordination of a monolayer of dialkyl-dithiophosphinate ligands to the surface which provides a hydrocarbon coating; this is important as it allows the materials to be processed by spin-coating. Doping the particles with a range of visible- and NIR-luminescent lanthanide ions allows sensitised luminescence to be achieved following excitation into the charge-transfer transition of the vanadate ion in the UV region; because the Ln(III) ions are in an inorganic matrix with only low-energy vibrational modes available, long luminescence lifetimes arise [27]. An exactly similar principle was used to achieve NIR luminescence from Nd(III), Er(III) and Yb(III) ions doped into soluble TiO_2 nanoparticles, where sensitisation occurs following excitation into the band edge of TiO_2 at <350 nm [28].

3. Work from the author’s group

Following the publication of papers by van Veggel and co-workers [18] and Parker and co-workers [16] in 2000 it was immediately obvious that this field was potentially very fertile—and largely unexplored. We were interested to try a systematic study of the syntheses and photophysical properties of different d–f combinations, but without having to make elaborate bridging ligands that required multi-step syntheses for each combination of metal ions. To that end we have investigated the two series of complexes described in the sections below, using a simple ‘complexes as ligands approach’ based on d-block chromophore complexes with one or more pendant binding sites to which lanthanide(III) fragments can bind strongly and quickly. This allows d-block and f-block components to be combined in an almost combinatorial manner with the minimum of synthetic difficulty.

3.1. Complexes based on polypyridine bridging ligands

For our first series of complexes we have exploited the fact that a wide range of $Ln(diketonate)_3$ complexes is easily available, usually as their eight-coordinate di-hydrates $Ln(diketonate)_3{\cdot}2H_2O$. Many of them are commercially available as NMR shift reagents. These complexes will bind a

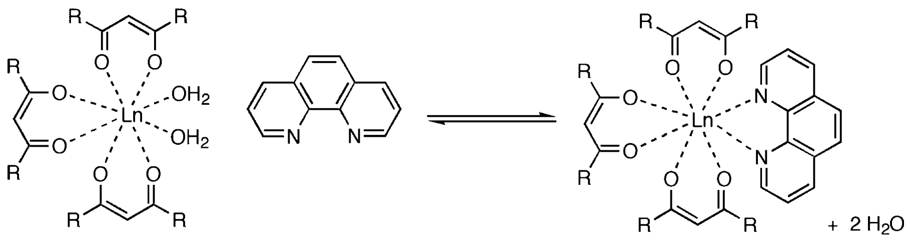

Scheme 2.

bidentate N-donor ligand such as bipyridine or phenanthroline with a high association constant, *ca.* $10^7\,M^{-1}$ in CH_2Cl_2 (Scheme 2) [29]. In donor solvents such as MeCN, alcohols or dmf, the diimine ligand is displaced and the adduct breaks up, but in CH_2Cl_2 the association is strong, and CH_2Cl_2 is a powerful enough solvent to dissolve readily a large range of metal complexes.

Our first proof-of-concept study used the known complexes [Re(bpym)(CO)$_3$Cl] (**XX**; bpym = 2,2′-bipyrimidine) and [Re(bppz)(CO)$_3$Cl] (**XXI**; bppz = 2,3-bis(2-pyridyl)pyrazine) as 'complex ligands' since each has a vacant diimine binding site [30]. Simple addition of one equivalent of a Ln(diketonate)$_3$ to a solution of the Re(I) complex in CH_2Cl_2 resulted in an immediate deepening of the colour of the Re(I)-diimine chromophore associated with binding of the Ln(diketonate)$_3$ fragment at the second binding site. Crystals grew readily by slow evaporation and the crystal structures of representative Re–Ln dyads **XX-Er** and **XXI-Nd** are in Fig. 3 [30]. In exactly the same way, complexes such as [PtCl$_2$(bppz)] (**XXII**), [Pt(PPh$_3$)$_2$(pdo)] (**XXIII**) (pdo = dianion of 5,6-phenanthroline-diol, coordinated as an *O*,*O*′-donor chelate) [31,32] [Pt(bpym)(CC–C$_6$H$_4$CF$_3$)$_2$] (**XXIV**) [33], and [Re(CO)$_3$ClL] (**XXV**) (where L is the bis-bidentate ligand py–CH=N–N=CH–py with two iminopyridine binding sites; py = 2-pyridyl) [34] could be used to prepare heterodinuclear d–f complexes (see Fig. 4 for representative crystal structures of lanthanide adducts of these complexes) simply by reaction with a Ln(diketonate)$_3\cdot 2H_2O$ in a low-polarity solvent.

Association constants for binding of the Ln(diketonate)$_3$ fragments to the diimine sites were readily determined by UV/vis spectroscopic titrations, monitoring the change in visible absorbance of the d-block chromophore as the Ln(diketonate)$_3$ fragment associated. Since association of the electropositive Ln(III) centre results in a reduction of the bridging ligand orbital energies, the general behaviour is that the MLCT absorptions of the d-block fragment are shifted to lower energy. The association constants in CH_2Cl_2 vary from about $10^4\,M^{-1}$ for complex **XXII-Ln** [32] to $10^5\,M^{-1}$ with **XXIV-Ln** [33] up to $>10^6\,M^{-1}$ with **XXIII-Ln** [32], according to the basicity of the diimine binding site. Pyrazine (in bppz) and bipyrimidine are weaker bases than pyridine, which is reflected in the lower association constants for lanthanide(III) complexes based on those fragments. It follows that at the concentrations typically used for solution luminescence measurements (at most $10^4\,M^{-1}$) there may be some significant dissociation of the Ln(diketonate)$_3$ fragment depending on the binding constant. However this is not a problem if we are examining d → f energy-transfer, because if we excite selectively into the d-block absorption band and monitor sensitized lanthanide-based NIR luminescence we will only be interrogating those molecules that remain intact. Also of course it is a simple matter to perform measurements on solid-state samples where dissociation ceases to be an issue.

For the series of complexes **XXII-Ln** and **XXIII-Ln** (Ln = Nd, Er, Yb in every case) excitation of the Pt(II) chromophore in the visible region (a Pt → diimine MLCT transition

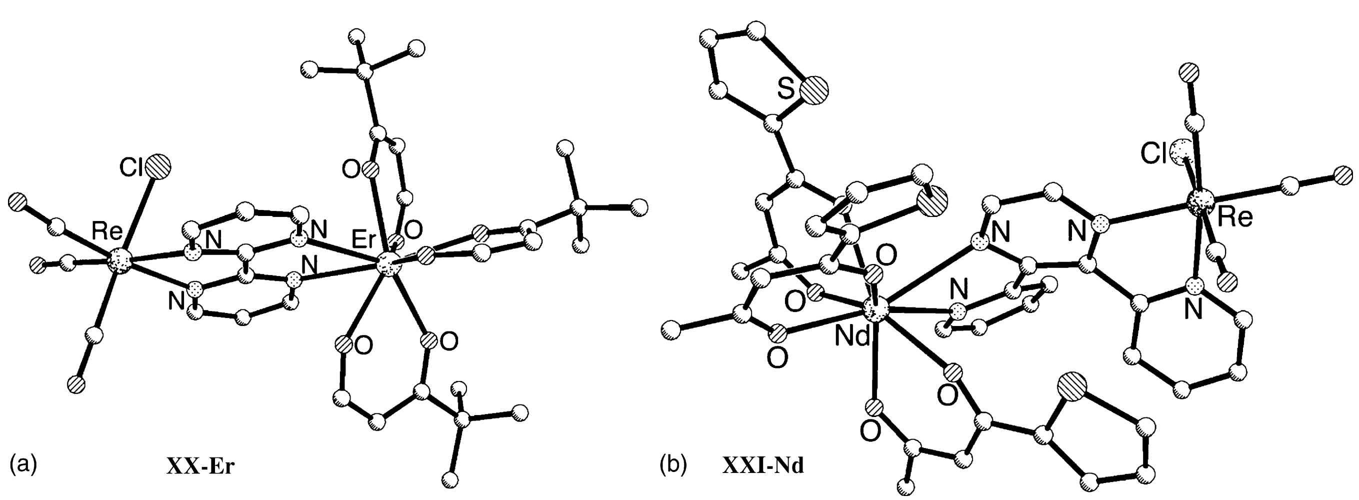

(a) **XX-Er**

(b) **XXI-Nd**

Fig. 3. Crystal structures of (a) [Re(CO)$_3$Cl(μ-bpym)Er(fod)$_3$], **XX-Er** (CF$_2$CF$_2$CF$_3$ side-chains on the fod ligands not shown for clarity); (b) [Re(CO)$_3$Cl(μ-bppz)Nd(tta)$_3$], **XXI**-Nd (F atoms on the tta ligands not shown for clarity).

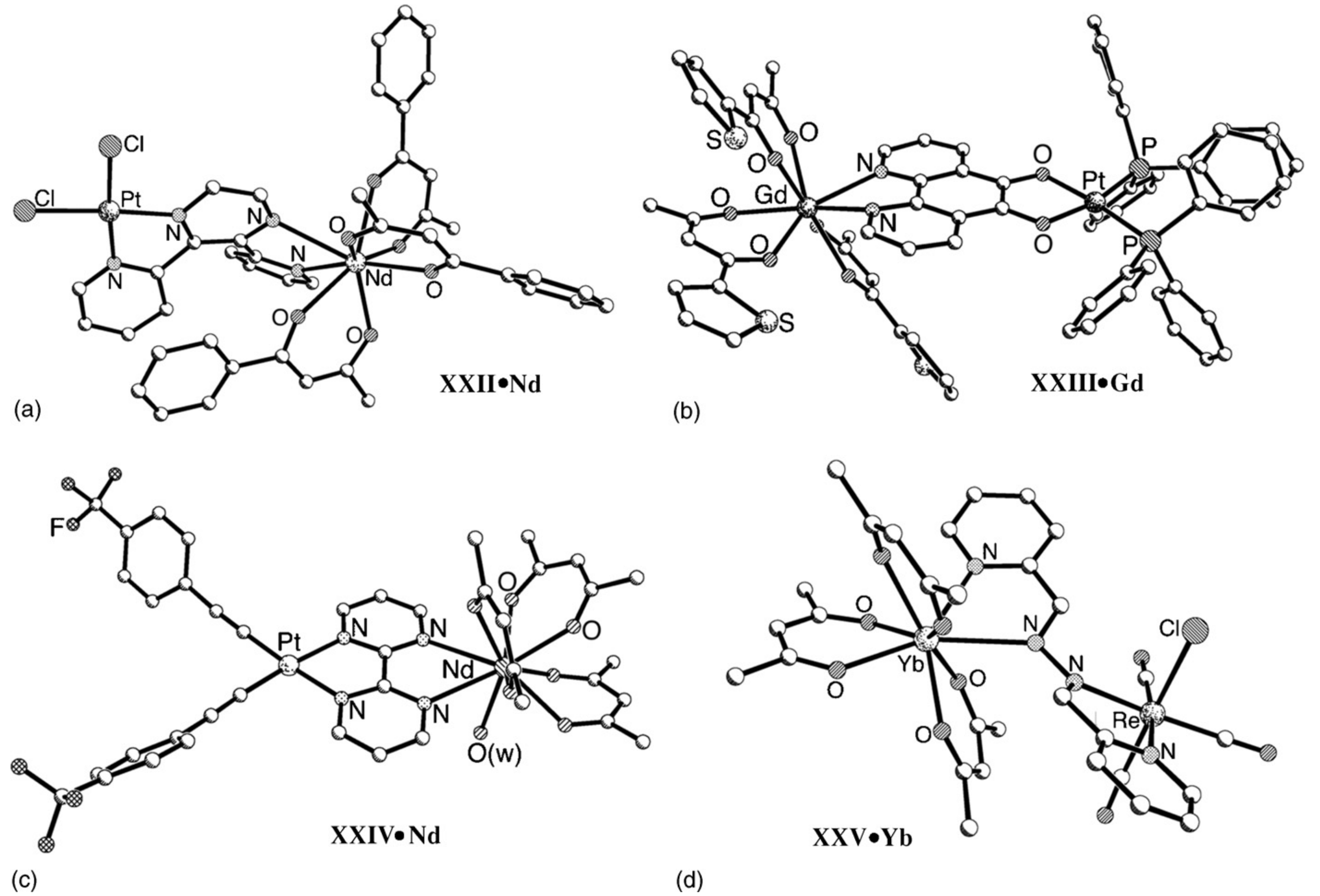

Fig. 4. Crystal structures of (a) [$PtCl_2$(μ-bppz)Nd$(btfa)_3$], **XXII-Nd** (F atoms on the btfa ligands omitted for clarity); (b) [$Pt(PPh_3)_2$(μ-pdo)Gd$(tta)_3$], **XXIII-Gd** (F atoms on the tta ligands not shown for clarity); (c) [$(hfac)_3$Nd(μ-bpym)Pt$(CC–C_6H4CF_3)_2$], **XXIV-Nd** (F atoms on the hfac ligands not shown for clarity); (d) [$Re(CO)_3Cl$(μ-py–CH=N–N=CH–py)Yb$(hfac)_3$], **XXV-Yb** (F atoms on the hfac ligands not shown for clarity).

in the first case at ≈440 nm; and a mixture of LLCT/LMCT/d–d transitions in the second at ≈500 nm) results in appearance of sensitized NIR luminescence at the characteristic wavelength of the relevant lanthanide(III) centre with typical lifetimes in the microsecond domain (≈10 μs for Yb; 2 μs for Er; 1 μs for Nd) [31,32]. No detectable rise-times for the luminescence implies energy-transfer that is fast on the timescale of the instrument used, *i.e.* $>10^8\,s^{-1}$, which may be ascribed to the relatively short metal–metal separations and the presence of conjugated, planar bridging ligands. The short d–f metal–metal separations (*ca*. 7.2 Å across bppz; 8.5 Å across pdo) will facilitate energy transfer by either Förster or Dexter mechanisms, whereas the electronic coupling provided by conjugated bridging ligands will facilitate specifically Dexter energy-transfer. It is important to note that this lanthanide-based luminescence can only arise by d → f energy-transfer because it arises from selective excitation of the d-block chromophore. Also, we found that solid (crystalline) samples showed similar behaviour, with the sensitized NIR luminescence having comparable lifetimes to what was observed in CH_2Cl_2 solution.

A limitation of the above systems is that since the d-block units are not themselves luminescent we have no easy way of determining the energy of the excited state which is acting as the energy donor. We can monitor d → f energy-transfer more readily – and also more quantitatively – if the d-block component is itself luminescent, as the energy-transfer process will be signaled by a reduction in the intensity and lifetime of this luminescence, which can allow the rate of energy transfer to be calculated. Thus, we can use the luminescence characteristics of the energy donor to monitor both the thermodynamics and kinetics of d → f energy-transfer. Accordingly we prepared [Pt(bpym)$(CC–C_6H_4CF_3)_2$] (**XXIV**) which in CH_2Cl_2 solution shows strong luminescence at 575 nm, with $\tau = 107$ ns; the ^{3}MLCT energy content is 19,300 cm^{-1} (as determined from the maximum of the luminescence in a frozen glass at 77 K) [33]. Addition of small portions of [$Ln(hfac)_3(H_2O)_2$] (Ln = Yb, Nd) resulted in progressive quenching of this luminescence as the Pt–Ln dyad formed (*cf*. crystal structure of **XXIV-Nd** in Fig. 4), with eventually the Pt-based luminescence being completely quenched. Pt → Yb energy transfer is clearly thermodynamically favourable since the only excited state of Yb(III), which must be the energy-acceptor, is $^2F_{5/2}$ which lies at 10,200 cm^{-1} above the ground state, much lower in energy than the ^{3}MLCT donor. For Nd(III) there are numerous possible energy-accepting levels lying below 19,300 cm^{-1} down to the emissive $^4F_{3/2}$ state at 11,300 cm^{-1}. On the basis of the spectroscopic overlap between the emission from the energy-donor and the absorption of the energy-acceptor we would expect that Pt → Nd energy-transfer should be faster than Pt → Yb energy transfer [following the pattern observed by van Veggel and co-workers in their $[Ru(bipy)_3]^{2+}$/Ln(III) dyads], because the numerous f–f excited states of Nd(III) should make it a more effective energy-acceptor [18]. However the complete quenching of Pt-based luminescence in both cases means that we can only say that energy-transfer is faster than the time resolution of the experimental setup (≈1 ns) in each case. This puts the Pt → Yb energy transfer rate at least four orders of magnitude faster than the $[Ru(bipy)_3]^{2+}$ → Yb energy-transfer that was observed in van Veggel's $[Ru(bipy)_3]^{2+}$/Yb(III) dyad [18], which is ascribable to a combination of a much shorter metal–metal separation and the presence of a conjugated ligand connecting the metal centres in **XXIV-Yb**.

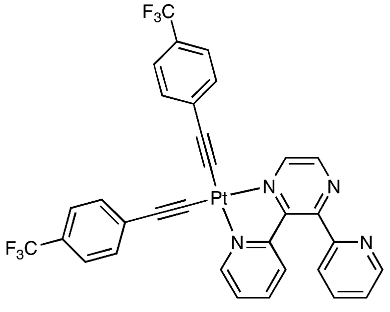

XXVI (see ref. 35)

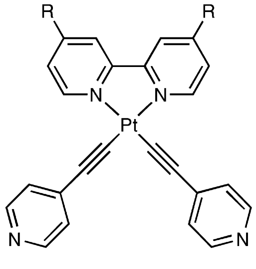

XXVII (R = H; see ref. 36)
XXVIII (R = ^{t}Bu; see ref. 36)

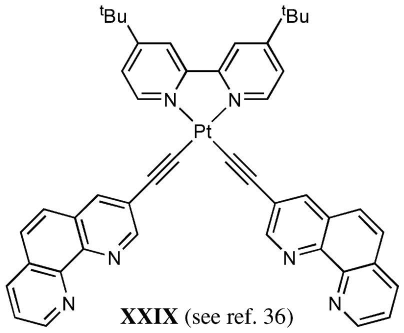

XXIX (see ref. 36)

By using longer spacers between the d-block and f-block components we could slow down the d → f energy-transfer to rates where it could be determined accurately on the basis of the reduction in lifetime of luminescence of the d-block energy-donor. If the unquenched luminescence lifetime of the energy donor is τ_u, and the lifetime in the presence of a lanthanide energy-acceptor is reduced to τ_q, then the energy-transfer rate K_{EnT} is just given by

$$k_{EnT} = \frac{1}{\tau_q} - \frac{1}{\tau_u} \tag{1}$$

This relies on being able to measure the 'quenched' lifetime τ_q, *i.e.* the quenching must not be complete, which it was with **XXFV-Yb**. The advantage of this is that it allows us to evaluate energy-transfer rates for different d–f combinations and start to develop a quantitative understanding of the phenomenon. In practice the 'unquenched' lifetime τ_u is not the luminescence lifetime of a d-block luminophore on its own, but of a Gd(III) adduct. Gd(III) cannot act as an energy acceptor in our d–f complexes because its lowest excited is too high in energy (>31,000 cm^{-1}, in the UV region), but it provides a similar steric and electrostatic contribution to the dyad as do other members of the lanthanide(III) series. Thus for a given d–f system the lifetimes of the d-block luminescence are measured (i) for the Gd(III) adduct (τ_u), and (ii) in the adduct with another lanthanide such as Yb(III) (τ_q). The rate of energy-transfer to Yb(III) is then given by application of Eq. (1).

$[Pt(bppz)(CC–C_6H_4CF_3)_2]$ (**XXVI**) was therefore used as an energy-donor; it luminesces at 600 nm in CH_2Cl_2 with $\tau = 250$ ns [35]. In the adducts $[(tta)_3Ln(\mu\text{-}bppz)Pt(CC–C_6H_4CF_3)_2]$ (**XXVI-Ln**), which form on addition of $[Ln(tta)_3(H_2O)_2]$ with an association constant of *ca.* 10^5 M^{-1}, the Pt···Ln separation is ≈7.2 Å, compared to ≈6.3 Å in the bipyrimidine-bridged complexes such as **XXIV-Ln**. When Ln = Gd the Pt(II)-based luminescence lifetime is reduced to 77 ns (the value of τ_u for (Eq. (1)). In the corresponding Pt–Nd and Pt–Yb adducts however the Pt-based emission lifetime was reduced to *ca.* 1 and 6 ns, respectively, giving values of Pt → Nd and Pt → Yb energy-transfer rates of ≈10^9 and 1.5×10^8 s^{-1}, respectively. Clearly Nd(III) is the more efficient energy-acceptor, in keeping with the presence of a large number of f–f excited states which are of an appropriate energy to quench the Pt(II)-based emission.

Complexes [Pt(bipy)(CC–4-pyridyl)] (**XXVII**) and [Pt($^t Bu_2$bipy)(CC–4-pyridyl)] (**XXVIII**) take this principle further by having an even greater separation between the Pt(II) luminescent centre and the pendant binding site (the 4-pyridyl groups), thereby slowing down Pt → Ln energy-transfer to the extent that it could be measured for all members of the series [36]. In solution these show strong luminescence at 508 and 520 nm, respectively, associated with Pt → bipy ^{3}MLCT emission. Given the proposed structure of the molecular square **XVI** it seemed possible that **XXVII** and **XXVIII**, which also have two pendant 4-pyridyl groups at approximately 90° to one another, could form similar squares on reaction with $Ln(diketonate)_3(H_2O)_2$ complexes. In fact the crystal structures of several such adducts revealed the structures of $\{$**XXVII**$\cdot Ln(tta)_3\}_\infty$ (**XXVII-Ln**) and $\{$**XXVIII**$\cdot Ln(hfac)_3\}_\infty$ (**XXVIII-Ln**) to be one-dimensional coordination polymeric chains with zigzag structures based on an alternating sequence of metal ions (Fig. 5), and Pt···Ln separations now extended to *ca.* 9.9 Å.

A significant feature of all of these structures was the involvement of all Pt(II) centres in short Pt···Pt contacts (3.34 Å), such that the energy-donor chromophore is not an isolated $\{Pt(bipy)(CCR)_2\}$ chromophore with an MLCT excited state, but a $\{Pt(bipy)(CCR)_2\}_2$ dimer (Fig. 5b) with an 'MMLCT' (metal–metal bond to ligand charge-transfer) excited state which luminescences at 635 nm, a considerably lower energy than the isolated mononuclear Pt(II) complexes (see Fig. 6). The effects of different lanthanides on the $\{Pt\}_2$-based emission in the isostructural series **XXVII·Ln** are also shown in Fig. 6; it is obvious how both the intensity and lifetime of the luminescence are decreased by energy-transfer, with $\{Pt\}_2$ → Ln energy-transfer rate constants becoming faster in the order Yb (2×10^6 s^{-1}) < Pr ≈ Er (4×10^7 s^{-1}) < Nd (≥10^8 s^{-1}). Very

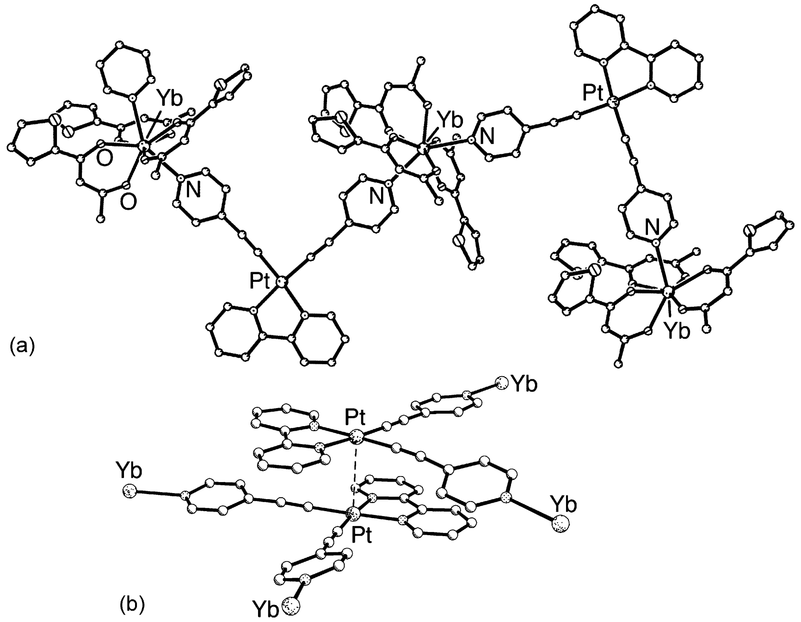

Fig. 5. Crystal structure of $\{\mathbf{XXVII}\cdot\mathrm{Yb(tta)_3}\}_\infty$ showing (a) the alternating chain structures, and (b) the Pt···Pt contacts between adjacent chains.

similar behaviour was observed for the **XXVIII·Ln** series. It is fairly obvious why Yb(III) should be the poorest energy-acceptor and Nd(III) the best, and this pattern is seen in many cases, as has been discussed earlier. Er(III) and Pr(III) clearly occupy an intermediate position. On the basis of availability of f–f excited states having an appropriate energy, we might expect $\{\mathrm{Pt}\}_2 \rightarrow \mathrm{Er}$ energy-transfer to be significantly faster than $\{\mathrm{Pt}\}_2 \rightarrow \mathrm{Pr}$ energy-transfer. However energy-transfer to the $^4F_{9/2}$ and $^4I_{9/2}$ levels of Er(III) is forbidden by both Förster and Dexter mechanisms. The former requires that $|\Delta J| = 2, 4$ or 6 at the lanthanide, and the latter requires that $|\Delta J| = 0$ or 1 (with the exception of $J = J' = 0$ which is forbidden) [37]. Population of the $^4F_{9/2}$ and $^4I_{9/2}$ levels of Er(III) would require $\Delta J = 3$ compared to the ground state, which is formally forbidden. Thus, Pr(III) and Er(III) are actually in a quite similar situation regarding their ability to be sensitised by energy-transfer, with one low-energy f–f state at $\approx$10,000 cm^{-1} and one higher-energy state [$^1D_2$ for Pr(III) at $\approx$17,500 cm^{-1}, and $^4S_{3/2}$ for Er(III) at $\approx$18,500 cm^{-1}. In all cases, quenching of the Pt-based luminescence following $\{\mathrm{Pt}\}_2 \rightarrow \mathrm{Ln}$ energy-transfer is accompanied by the usual sensitised NIR luminescence from the lanthanides at their characteristic wavelengths and with typical lifetimes [36].

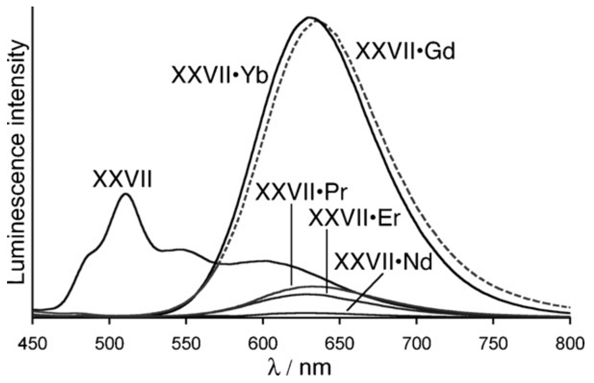

Fig. 6. Solid-state emission spectra in the visible region of complex **XXVII** and its adducts with various $\{\mathrm{Ln(tta)_3}\}$ groups (see Fig. 5 for crystal structure). Note the relatively high energy luminescence from **XXVII** on its own in which there are no Pt···Pt interactions in the solid state; this is accordingly ^{3}MLCT-based emission from a monomer. The $\{\mathrm{Ln(tta)_3}\}$ adducts all have a short Pt···Pt contact in the solid state (Fig. 5b) resulting from lower-energy luminescence from a $\{\mathrm{Pt_2}\}$ ^{3}MMLCT excited state. The degree of quenching of this depends on the lanthanide ion; see main text.

The comparison of these with $\mathbf{XXIX}\cdot\{\mathrm{Ln(hfac)_3}\}_2$ (**XXIX-Ln**) is interesting. Complex **XXIX** contains essentially the same $\{\mathrm{Pt(bipy)(CCR)_2}\}$ chromophore as **XXVII** and **XXVIII**, but with two pendant bidentate 1,10-phenanthrolinyl binding sites; accordingly it forms trinuclear adducts in which a $\{\mathrm{Ln(hfac)_3}\}$ fragment binds at each phenanthroline site [36]. In this case however there is no Pt···Pt interaction in the solid state (or solution) and the ^{3}MLCT luminescence of the isolated $\{\mathrm{Pt(bipy)(CCR)_2}\}$ chromophore is now at 526 nm (*cf.* 635 nm for the **XXVII·Ln** and **XXVIII·Ln** series due to the Pt···Pt association, Fig. 6). As a consequence of this the order of Pt → Ln energy-transfer rate constants to lanthanides is altered. In the series of adducts with Gd, Yb, Er and Nd the Pt(II)-based luminescence lifetimes were 835, 17, 7, and $\approx$1 ns, giving Pt → Ln energy-transfer rate constants in the order Yb (6×10^7 s^{-1}) < Nd (1.4×10^8 s^{-1}) < Er ($\approx 10^9$ s^{-1}). In this series we now see that Er(III) is a better energy-acceptor than Nd(III), resulting in a greater degree of quenching of the excited state of the Pt(II) chromophore. This may be explained with reference to Fig. 7. The higher energy of the Pt-based ^{3}MLCT emission of **XXIX** means that it now overlaps effectively with the principal Er(III)-based absorption such that donor/acceptor spectroscopic overlap between Pt(II) and Er(III) is much improved compared to the situation in **XXVII·Ln** and **XXVIII·Ln**, where the $\{\mathrm{Pt}\}_2$-based luminescence was lower in energy and overlapped more effectively

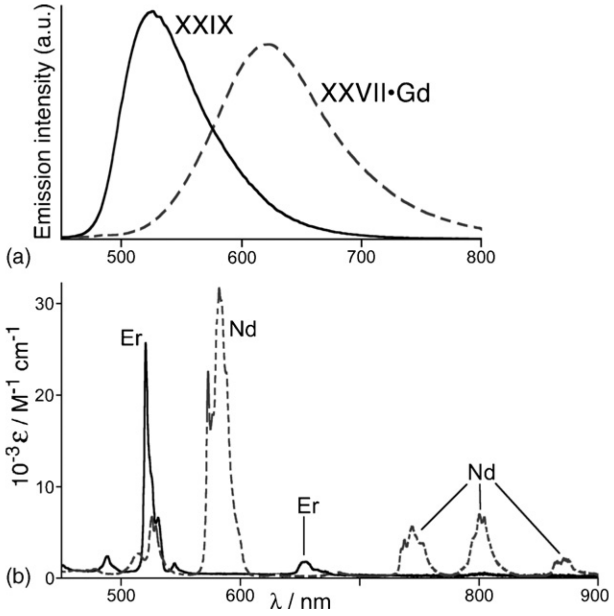

Fig. 7. (a) Emission profiles from **XXIX** (^{3}MLCT based, in solution; solid line) and [**XXVII**·Gd(tta)$_3$]$_\infty$ (^{3}MMLCT based, solid state; dashed line); (b) absorption spectra of [Ln(hfac)$_3$(phen)] in CH_2Cl_2 solution (Ln = Er, solid line; Nd, dashed line). The correspondences between the emission maximum of **XXIX** and absorption of Er(III), and the emission maximum of [**1**·Gd(tta)$_3$]$_\infty$ and the absorption of Nd(III), are obvious.

with Nd(III)-based f–f transitions. Thus Nd(III) is more effective than Er(III) as an energy-acceptor in the series **XXVII·Ln** and **XXVIII·Ln**, whereas Er(III) is more effective than Nd(III) as an energy-acceptor in the series **XXIX·Ln** [36]. Although this observation is a consequence of well-understood rules for photoinduced energy-transfer, it is gratifying to see it demonstrated so clearly in d–f dyads, and it will clearly be possible to use this principle to optimize combinations of d-block energy-donor with f-block acceptor to achieve the most effective sensitization of NIR luminescence.

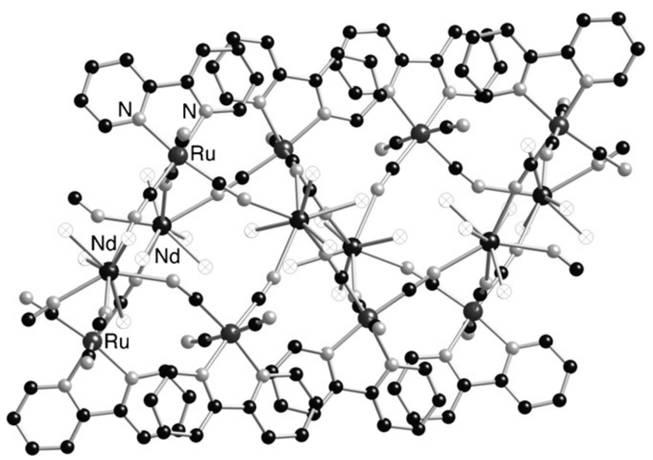

Fig. 8. Two-dimensional cyanide-bridged sheet structure of the coordination network [{Ru(bipy)(CN)$_4$}$_3${Nd(H_2O)$_4$}$_2$]·11H_2O. The O atoms of waters coordinated to Nd are shown hollow; the N atoms are filled paler-coloured spheres.

3.2. Cyanide-bridged d–f coordination networks

Luminescent cyanoruthenate complexes such as [Ru(bipy)(CN)$_4$]$^{2-}$ and its relatives with other diimine ligands are also ideal from both a structural and a photophysical point of view to prepare d–f hybrid systems [38]. As with [Ru(bipy)$_3$]$^{2+}$ the ^{3}MLCT excited state is (in protic media) strong and long-lived; and the anionic chromophore associates with metal cations, including lanthanides, *via* bridging Ru–CN–Ln interactions to have a range of elaborate coordination networks in which the Ru···Ln separations are in the range 5.3–5.6 Å (see Fig. 8 for one example) [39,40]. Preparation is trivially simple, just involving slow crystallization of K_2[Ru(bipy)(CN)$_4$]

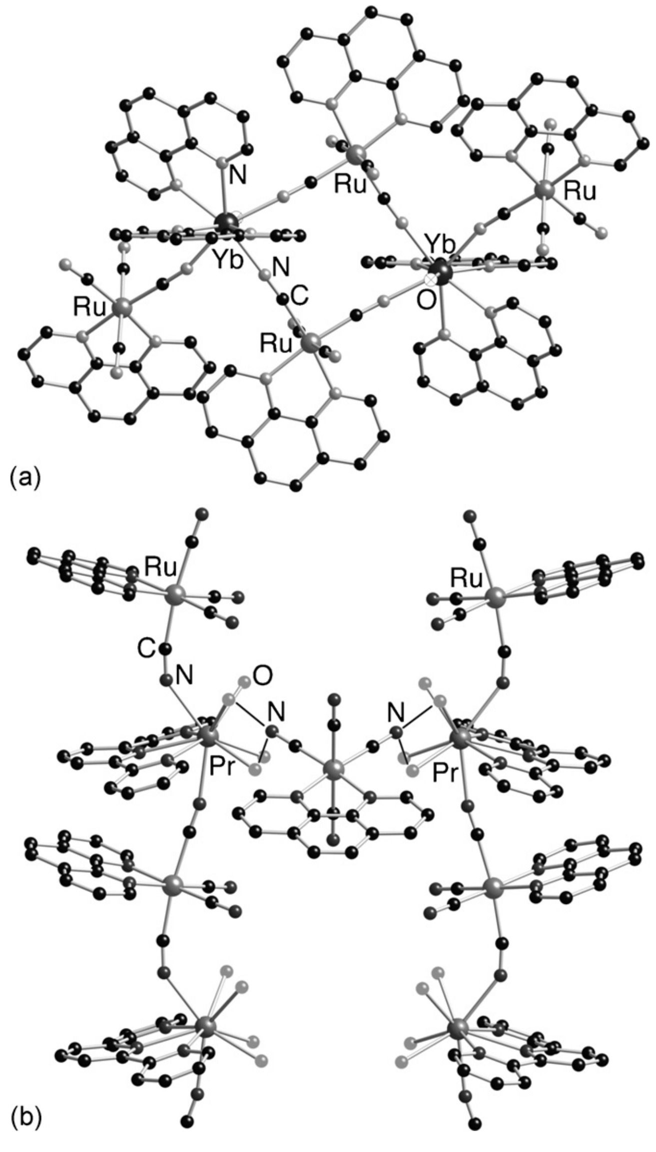

Fig. 9. Two structures of ternary [Ru(phen)(CN)$_4$]$^{2-}$/Ln(III)/polypyridine ligand networks in which an additional polypyridyl ligand (1,10-phenanthroline or 2,2′:6′,2″′-terpyridine) blocks some of the coordination sites of the Ln(III) centre in an attempt to minimise non-radiative deactivation pathways associated with coordinated water and/or cyanide ligands. (a) {[Ru(phen)(CN)$_4$]$_2$-[Yb(phen)$_2$(H_2O)]K(H_2O)$_{14}$}$_2$; (b) {[Ru(phen)(CN)$_4$]$_3$[Pr(terpy)(H_2O)$_3$]$_2$·12.5H_2O}$_\infty$ (CN···HOH hydrogen-bonds are indicated by solid lines between N and O atoms).

with Ln(III) salts from aqueous solution. The photophysical properties of $[Ru(bipy)(CN)_4]^{2-}$ and its relatives have been reviewed recently in this journal and do not need to be rehearsed again [38]. That review also contained a brief account of the structural and photophysical characterization of $[Ru(bipy)(CN)_4]^{2-}/Ln^{3+}$ coordination networks [39] (*cf.* Fig. 8), of which the most significant feature for the purposes of this article was the rates of Ru → Ln energy-transfer to different lanthanides: these varied in the order Yb ($3 \times 10^6\,s^{-1}$) < Er ($10^7\,s^{-1}$) < Pr ($4 \times 10^7\,s^{-1}$) < Nd ($2 \times 10^8\,s^{-1}$), with Ru → Yb energy-transfer being the slowest and Ru → Nd energy-transfer being the fastest, in agreement with the general pattern discussed above for many d–f systems in which the d-block component has its luminescence in the 600–650 nm region. In these cyanide-bridged networks the lifetimes of the sensitized lanthanide-based NIR luminescence were much shorter than in the $\{Ln(diketonate)_3(NN)\}$ luminophores discussed in the previous section. For example the Yb-based emission is reduced from ≈10 μs to a few hundred nanoseconds, even if the water molecules in the Yb(III) coordination sphere and in the lattice were replaced by D_2O ligands. Although efficient quenching of NIR luminescence in lanthanides is usually associated with high-energy (C–H and O–H, at ≈3000 cm^{-1}) oscillators close to the metal centre, in these networks we suggest that the high degree of cross-linking via the cyanide ligands allows the excited state energy of the Ln(III) centre to be dispersed as lattice phonons particularly effectively even via the relatively low-energy cyanide oscillators (≈2000 cm^{-1}) [39].

Following these initial results we have recently investigated two new avenues for this work. Firstly, in order to make Ru/Ln coordination networks in which the sensitized NIR luminescence lifetime is longer, we have attempted to reduce the degree of cyanide-based cross-linking by adding additional ligands such as 1,10-phenanthroline or 2,2′:6′,2″-terpyridine which will bind to the Ln(III) cations and hence reduce the number of sites available for coordination of bridging cyanides. Two examples of such structures are shown in Fig. 9 [41]. In $\{[Ru(phen)(CN)_4]_3[Pr(terpy)(H_2O)_3]_2 \cdot 12.5H_2O\}_\infty$, charge balance is provided by the 3:2 ratio of $[Ru(phen)(CN)_4]^{2-}$ to Pr^{3+} units in the asymmetric unit. The main feature of the structure is the presence of two crystallographically independent ladder-like one-dimensional chains oriented along the *a*-axis, of which one is shown in Fig. 9. Each ladder consists of two strands based on alternating Ru(II) and Pr(III) centres connected by a cyanide bridge to give a quasi-linear chain; two such parallel chains are connected by additional cyanide cross-pieces (which form the 'rungs' of the ladder) which likewise connect Ru(II) and Pr(III) centres. Importantly the presence of a terpyridyl ligand coordinated to each Pr(III) means that there are now only three bridging cyanides (and three D_2O ligands). In $\{[Ru(phen)(CN)_4]_2[Yb(phen)_2(H_2O)]K(H_2O)_{14}\}_2$ the −4 charge of two independent $[Ru(phen)(CN)_4]^{2-}$ dianions is offset by one Yb(III) centre and one K^+ ion; the structure consists of discrete hexanuclear units based on a $Ru_2Yb_2(\mu\text{-}CN)_4$ ring, with two additional $[Ru(phen)(CN)_4]^{2-}$ units pendant from the ring via cyanide bridges to each of the Yb(III) centres. The Yb(III) centres are eight-coordinate from two coordinated phen ligands, three bridging cyanides, and one water ligand, so the presence of the additional phen ligands has again reduced the degree of cyanide-based cross linking. It is hoped that this will result in increased NIR emission lifetimes following excitation of the $[Ru(phen)(CN)_4]^{2-}$ chromophores; such studies are in progress.

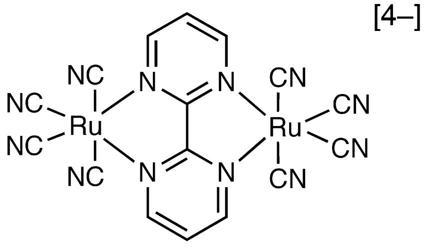

XXX (see refs. 42, 43)

Secondly, we have made more elaborate Ru/Ln networks based on dinuclear and trinuclear complexes $[\{Ru(CN)_4\}_2(\mu\text{-}bpym)]^{4-}$ (**XXX**; bpym = 2,2′-bipyrimidine) [42,43] and $[\{Ru(CN)_4\}_3(\mu\text{-}HAT)]^{6-}$ (**XXXI**; HAT = hexaaza-triphenylene) [44]. From a structural point of view these are interesting because they provide 'nodes' of much higher potential connectivity (up to 12 connections) than can be achieved using mononuclear cyanometallate complexes in which the highest connectivity is normally six, in Prussian-blue type cubic structures. From a photophysical point of view, **XXX** and **XXXI** have more intense MLCT absorptions at lower energy than mononuclear species such as $[Ru(bipy)(CN)_4]^{2-}$ and are therefore more effective light-harvesting groups which should allow NIR luminescence to be sensitised using a greater part of the visible spectrum for sensitisation. For example, **XXXI** has its MLCT absorption maximum at 524 nm in aqueous solution, with an extinction coefficient of >30,000 $M^{-1}\,cm^{-1}$; the tail of the absorption band extends out to 700 nm, making it a strong absorber across most of the visible spectrum.

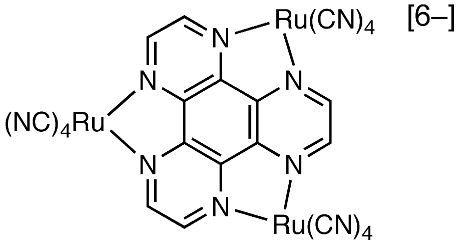

XXXI (see ref. 44)

The structures of $[\textbf{XXX}][Nd(NO_3)(H_2O)_5]_2 \cdot 3H_2O$ and $[\textbf{XXX}][Yb(H_2O)_6]_{0.5}[Yb(H_2O)_4](NO_3)_{0.5} \cdot 8H_2O$ are shown in Fig. 10; the former has a one-dimensional ladder-like structures in which the bipyrimidine ligands from the cross-pieces, whereas the latter is a three-dimensional network in which two-dimensional sheets of $Ru_2Yb_2(\mu\text{-}CN)_4$ diamonds are connected via cyanide bridges to Yb(III) ions between the layers. The structure of $Nd_2[\textbf{XXXI}] \cdot 23H_2O$ (Fig. 11) consists of two-dimensional sheets in which the six cyanides of each complex anion **XXXI** that are in the same plane as the HAT ligand all coordinate to Nd(III) centres. Each Nd(III) is nine-coordinate, from

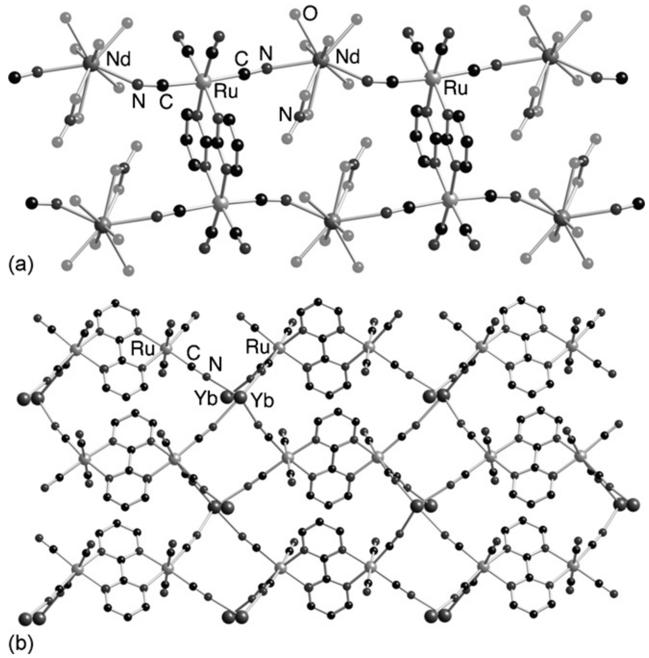

Fig. 10. Structures of (a) [**XXX**][$Nd(NO_3)(H_2O)_5]_2 \cdot 3H_2O$, and (b) [**XXX**][$Yb(H_2O)_6]_{0.5}[Yb(H_2O)_4](NO_3)_{0.5} \cdot 8H_2O$ (with coordinated water molecules not shown for clarity).

five water and four cyanide ligands, with three of the cyanide ligands coming from ‘in-plane’ **XXXI** units. These sheets are held together by two additional bridging cyanide interactions from two of the six axial cyanides, which connect to Nd(III) centres in the layers above and below. Each **XXXI** unit accordingly uses eight of its twelve cyanide ligands in bridging interactions to propagate the network.

The polynuclear complex anions **XXX** and **XXXI** are very weakly or non-luminescent in both the solution and the solid state so we cannot use time-resolved measurements of their residual luminescence lifetimes to quantify Ru → Ln energy-transfer rates. However in the complexes of **XXX** with Nd(III) and Yb(III), and of **XXXI** with Nd(III), excitation into the cyanoruthenate absorption manifold afforded sensitised NIR luminescence from the lanthanide(III) centres at their characteristic wavelengths, although the NIR luminescence lifetimes were again relatively short due to the presumed effects of cyanide cross-linking in facilitating non-radiative deactivation of the f–f excited states.

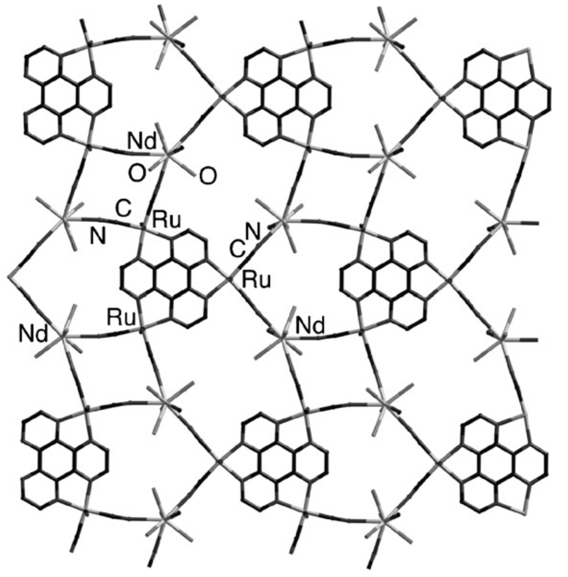

Fig. 11. Structure of one of the two-dimensional layers in Nd_2[**XXXI**]$\cdot 23H_2O$.

4. Conclusions

This is a field which has really taken off in recent years; all of the results from the author’s group, and nearly all of the results from other groups working in the area, date from the year 2000 or after. The ability of strongly absorbing d-block chromophores to sensitise low-energy f–f states of NIR emitting lanthanides has been well established and important criteria for optimising energy-transfer have been established. Major goals now include (i) using the tricks that have been developed for dramatically extending the NIR luminescence lifetime (see Section 1) in other situations, and (ii) making water-stable d–f systems which allow long wavelength excitation (700 nm or longer) to be used to generate long-lived NIR luminescence for biological imaging applications.

Acknowledgements

I would like to thank the many talented members of my group who have carried out the work reviewed in Section 3 (Drs. Nail Shavaleev, Graham Davies, Tanya Ronson, Ted Lazarides, Tom Miller, Jean-Manuel Herrera and Svetlana Baca); and my collaborators who have performed numerous invaluable measurements involving photophysics (Drs. Nicola Armaroli, Simon Pope, and Prof. Steven Faulkner) and X-ray crystallography (Drs. John Jeffery, Zöe Bell, and Mr. Harry Adams).

References

[1] (a) J. Silver, in: M.D. Ward (Ed.), Comprehensive Coordination Chemistry, vol. 9, 2nd ed., Elsevier, Oxford, 2004, p. 689;
(b) R.C. Evans, P. Douglas, C.J. Winscom, Coord. Chem. Rev. 250 (2006) 2093.

[2] (a) O.S. Wolfbeis, A. Durkop, M. Wu, Z.H. Lin, Angew. Chem., Int. Ed. 41 (2002) 4495;
(b) J.P. Leonard, T. Gunnlaugsson, J. Fluoresc. 15 (2005) 585;
(c) S. Pandya, J.H. Yu, D. Parker, Dalton Trans. (2006) 2757;
(d) K. Hanaoka, K. Kikuchi, H. Kojima, Y. Urano, T. Nagano, J. Am. Chem. Soc. 126 (2004) 12470.

[3] (a) S. Faulkner, S.J.A. Pope, B.P. Burton-Pye, Appl. Spectrosc. Rev. 40 (2005) 1;
(b) G.R. Motson, J.S. Fleming, S. Brooker, Adv. Inorg. Chem. 55 (2004) 361;
(c) S. Faulkner, J.L. Matthews, in: M.D. Ward (Ed.), Comprehensive Coordination Chemistry, vol. 9, 2nd ed., Elsevier, Oxford, 2004, p. 913.

[4] A.P. Bassett, R. van Deun, P. Nockemann, P.B. Glover, B.M. Kariuki, K. van Hecke, L. van Meervelt, Z. Pikramenou, Inorg. Chem. 44 (2005) 6140.

[5] G. Mancino, A.J. Ferguson, A. Beeby, N.J. Long, T.S. Jones, J. Am. Chem. Soc. 127 (2005) 524.

[6] D. Imbert, M. Cantuel, J.-C.G. Bünzli, G. Bernardinelli, C. Piguet, J. Am. Chem. Soc. 125 (2003) 15698.

[7] S. Torelli, D. Imbert, M. Cantuel, G. Bernardinelli, S. Delahaye, A. Hauser, J.-C.G. Biinzli, C. Piguet, Chem. Eur. J. 11 (2005) 3228.
[8] J.W. Stoudam, G.A. Hebbink, J. Huskens, F.C.J.M. van Veggel, Chem. Mater. 15 (2003) 4604.
[9] (a) S. Lis, M. Elbanowski, B. Makowska, Z. Hnatejko, J. Photochem. Photobiol. A: Chem. 150 (2002) 233;
(b) N. Sabbatini, M. Guardigli, J.-M. Lehn, Coord. Chem. Rev. 123 (1993) 201.
[10] G.A. Hebbink, S.I. Klink, L. Grave, P.G.B.O. Alink, F.C.J.M. van Veggel, Chem. Phys. Chem. 3 (2002) 1014.
[11] M.H.V. Werts, N. Nerambourg, D. Pélégry, Y. Le Grand, M. Blanchard-Desce, Photochem. Photobiol. Sci. 4 (2005) 531.
[12] L.-M. Fu, X.-F. Wen, X.-C. Ai, Y. Sun, Y.-S. Wu, J.-P. Zhang, Y. Wang, Angew Chem., Int. Ed. 44 (2005) 747.
[13] G.A. Hebbink, L. Grave, L.A. Woldering, D.N. Reinhoudt, F.C.J.M. van Veggel, J. Phys. Chem. A 107 (2003) 2483.
[14] M.P.O. Wolbers, F.C.J.M. van Veggel, F.G.A. Peters, E.S.E. van Beelen, J.W. Hofstraat, F.A.J. Geurts, D.N. Reinhoudt, Chem. Eur. J. 4 (1998) 772.
[15] N.M. Shavaleev, S.J.A. Pope, Z.R. Bell, S. Faulkner, M.D. Ward, Dalton Trans. (2003) 808.
[16] A. Beeby, R.S. Dickins, S. Fitzgerald, L.J. Govenlock, C.L. Maupin, D. Parker, J.P. Riehl, G. Siligardi, J.A.G. Williams, Chem. Commun. (2000) 1183.
[17] R.F. Ziessel, G. Ulrich, L. Charbonniere, D. Imbert, R. Scopelliti, J.-C.G. Bünzli, Chem. Eur. J. 12 (2006) 5060.
[18] (a) S.I. Klink, H. Keizer, F.C.J.M. van Veggel, Angew Chem. Int. Ed. 39 (2000) 4319;
(b) S.I. Klink, H. Keizer, H.W. Hofstraat, F.C.J.M. van Veggel, Synth. Met. 127 (2002) 213.
[19] S.J.A. Pope, B.J. Coe, S. Faulkner, Chem. Commun. (2004) 1551.
[20] S.J.A. Pope, B.J. Coe, S. Faulkner, R.H. Laye, Dalton Trans. (2005) 1482.
[21] S.J.A. Pope, B.J. Coe, S. Faulkner, E.V. Bichenkova, X. Yu, K.T. Douglas, J. Am. Chem. Soc. 126 (2004) 9490.
[22] S.J.A. Pope, B.P. Burton-Pye, R. Berridge, T. Khan, P.J. Skabara, S. Faulkner, Dalton Trans. (2006) 2907.
[23] P.D. Beer, F. Szemes, P. Passaniti, M. Maestri, Inorg. Chem. 43 (2004) 3965.
[24] P.B. Glover, P.R. Ashton, L.J. Childs, A. Rodger, M. Kercher, R.M. Williams, L. De Cola, Z. Pikramenou, J. Am. Chem. Soc. 125 (2003) 9918.
[25] D. Guo, C. Duan, F. Lu, Y. Hasegawa, Q. Meng, S. Yanagida, Chem. Commun. (2004) 1486.
[26] H.-B. Xu, L.-X. Shi, E. Ma, L.-Y. Zhang, Q.-H. Wei, Z.-N. Chen, Chem. Commun. (2006) 1601.
[27] J.W. Stouwdam, M. Raudsepp, F.C.J.M. van Veggel, Langmuir 21 (2005) 7003.
[28] J.W. Stouwdam, F.C.J.M. van Veggel, Chem. Phys. Chem. 5 (2004) 743.
[29] (a) K. Iftikhar, M. Sayeed, N. Ahmad, Inorg. Chem. 21 (1982) 80;
(b) W.H. Watson, R.J. Williams, N.R. Stemple, J. Inorg. Nucl. Chem. 34 (1982) 501;
(c) S. Yajima, Y. Hasegawa, Bull. Chem. Soc. Jpn. 71 (1998) 2825.
[30] N.M. Shavaleev, Z.R. Bell, M.D. Ward, J. Chem. Soc., Dalton Trans. (2002) 3925.
[31] N.M. Shavaleev, L.P. Moorcraft, S.J.A. Pope, Z.R. Bell, S. Faulkner, M.D. Ward, Chem. Commun. (2003) 1134.
[32] N.M. Shavaleev, L.P. Moorcraft, S.J.A. Pope, Z.R. Bell, S. Faulkner, M.D. Ward, Chem. Eur. J. 9 (2003) 5283.
[33] N.M. Shavaleev, G. Accorsi, D. Virgili, Z.R. Bell, T. Lazarides, G. Calogero, N. Armaroli, M.D. Ward, Inorg. Chem. 44 (2005) 61.
[34] N.M. Shavaleev, Z.R. Bell, G. Accorsi, M.D. Ward, Inorg. Chim. Acta 351 (2003) 159.
[35] F. Kennedy, N.M. Shavaleev, Z.R. Bell, T. Koullourou, S. Faulkner, M.D. Ward, Dalton Trans., submitted for publication.
[36] T.K. Ronson, T. Lazarides, H. Adams, S.J.A. Pope, D. Sykes, S. Faulkner, S.J. Coles, M.B. Hursthouse, W. Clegg, R.W. Harrington, M.D. Ward, Chem. Eur. J., in press.
[37] G.F. de Sá, O.L. Malta, C. de Mello Donegá, A.M. Simas, R.L. Longo, P.A. Santa-Cruz, E.F. da Silva Jr., Coord. Chem. Rev. 196 (2000) 165.
[38] M.D. Ward, Coord. Chem. Rev. 250 (2006) 3128.
[39] (a) G.M. Davies, S.J.A. Pope, H. Adams, S. Faulkner, M.D. Ward, Inorg. Chem. 44 (2005) 4656;
(b) T.A. Miller, J.C. Jeffery, M.D. Ward, H. Adams, S.J.A. Pope, S. Faulkner, Dalton Trans. (2004) 1524.
[40] H. Adams, W.Z. Alsindi, G.M. Davies, M.B. Duriska, T.L. Easun, H.E. Fenton, J.-M. Herrera, M.W. George, K.L. Ronayne, X.-Z. Sun, M. Towrie, M.D. Ward, Dalton Trans. (2006) 39.
[41] S.G. Baca, H. Adams, M.D. Ward, Cryst. Eng. Commun. 8 (2006) 635.
[42] J.-M. Herrera, S. Baca, H. Adams, M.D. Ward, Polyhedron 25 (2006) 869.
[43] J.-M. Herrera, S.J.A. Pope, H. Adams, S. Faulkner, M.D. Ward, Inorg. Chem. 45 (2006) 3895.
[44] J.-M. Herrera, M.D. Ward, H. Adams, S.J.A. Pope, S. Faulkner, Chem. Commun. (2006) 1851.